

Kinetic electron emission for planar versus axial surface channeling of He atoms and ions

H. Winter,* K. Maass, and S. Lederer

Institut für Physik, Humboldt Universität zu Berlin, Brook-Taylor-Strasse 6, D-12489 Berlin, Germany

HP. Winter and F. Aumayr

Institut für Allgemeine Physik, Technische Universität Wien, Wiedner Hauptstrasse 8-10, A-1040 Vienna, Austria

(Received 16 September 2003; published 24 February 2004)

Fast He^+ ions and He^0 atoms are scattered under grazing incidence from a clean and flat Al(111) surface. The target current recorded as function of azimuthal angle with respect to the surface orientation is enhanced for scattering along low-index crystallographic directions. Coincident studies on the number of electrons emitted per ion impact allow us to explore this effect. We find that the increase of the total electron yield for surface channeling along low-index directions stems primarily from projectiles with trajectories in the subsurface region and the consequent emission of a substantially larger number of electrons.

DOI: 10.1103/PhysRevB.69.054110

PACS number(s): 79.20.Rf, 61.85.+p, 79.60.Bm

When fast atomic projectiles collide with a crystal target, the crystallographic orientation of the sample relative to the incident beam generally affects their trajectories and interactions with the solid. This holds, in particular, for impact along low-index directions with respect to atomic planes or strings. This phenomenon, named “channeling,” was revealed in computer simulations¹ and experiments showing enhanced ranges for ions into thin crystal foils.² Projectile trajectories, energy loss, or electron emission are modified under channeling conditions which was investigated in past decades.³ One distinguishes between the two regimes of planar and axial channeling, i.e., a steering of projectiles by crystal planes and strings of target atoms, respectively.

A particular regime of channeling is met for the scattering of atomic projectiles from a solid surface under a grazing angle of incidence. Then the interaction with the solid proceeds under (semi)planar surface channeling^{4,5} at the topmost surface layer resulting in specular reflection of projectiles with well-defined trajectories. From the variety of interesting phenomena and effects studied in this regime of surface scattering in recent years⁶ electron emission induced by grazing ion impact shows a number of new features.^{7–11} An interesting effect in this respect is observed, when projectiles are scattered along low-index crystallographic directions of the surface plane resulting in the additional steering by strings of atoms in the topmost surface layer (“axial surface channeling”). Electron emission is found to depend on the azimuthal settings of the target surface.^{12,13}

As a prominent example, one mostly observes an enhancement of electron yields, whenever the direction of the incident ion beam coincides with low-index directions in the surface plane.^{7,8,10} Such higher electron emission yields for surface scattering can simply be detected by an enhanced target current. This feature allows one to perform an online azimuthal alignment of the crystal surface and, since channeling is affected by crystal defects, it can also be used as a surface analytical tool.⁶ Recently, it was shown that the preferential emission of electrons under axial surface channeling can be applied to study the structure of surfaces and, in particular, ultrathin films (“ion beam triangulation”).¹⁴ Directions of closed-packed rows in the surface layer of substrate

or thin film can be identified by peaks of the target current for an azimuthal rotation of the target, and real-space information on the surface structure can be derived. As a result, we mention a new structural model for the $c(12 \times 8)$ phase of a Mn bilayer epitaxially grown on Cu(001).¹⁴

The enhanced emission of electrons observed for the transition from planar to axial surface channeling was interpreted in a straightforward manner: For axial channeling, i.e., scattering along strings of surface atoms, projectiles enter regions of higher electron densities and have longer trajectories.^{7,8,10} As recent work on this problem, we cite work by Andou *et al.*¹⁵ on grazing scattering of 500 keV protons from a KCl(001) surface. From the comparison of electron spectra recorded in coincidence with scattered projectiles with computer simulations, enhanced electron emission under axial channeling was attributed to longer projectile trajectories.

We will demonstrate that, in particular, for low and medium energy ion scattering the interpretation for this effect is more intricate. In our work we have studied for 16 keV He projectiles scattered from an Al(111) surface the number of emitted electrons for the transition from planar to axial channeling. From spectra recorded in *coincidence* and *noncoincidence* with scattered projectiles we deduce aspects concerning the interpretation of this problem. Our data provide clear evidence that the enhanced emission of electrons is closely related to projectiles, which have penetrated into the subsurface region with clearly enhanced yields for kinetic emission of electrons. This mechanism can be exploited in terms of enhanced signal-to-background ratios in ion beam triangulation.

In our experiments, He^0 atoms and He^+ ions with an energy of 16 keV are scattered under a grazing angle of incidence $\Phi_{in} = 1.9^\circ$ from a well-prepared atomically clean and flat Al(111) surface kept at a base pressure of some 10^{-11} mbar and at room temperature. Projectiles reflected from the surface are recorded in coincidence with electron multiplicities for each scattering event by means of an electron number detector [surface barrier detector (SBD) biased to + 25 kV, detector pulse heights proportional to the number of ejected electrons per projectile impact on the surface¹⁶]. Pulsed

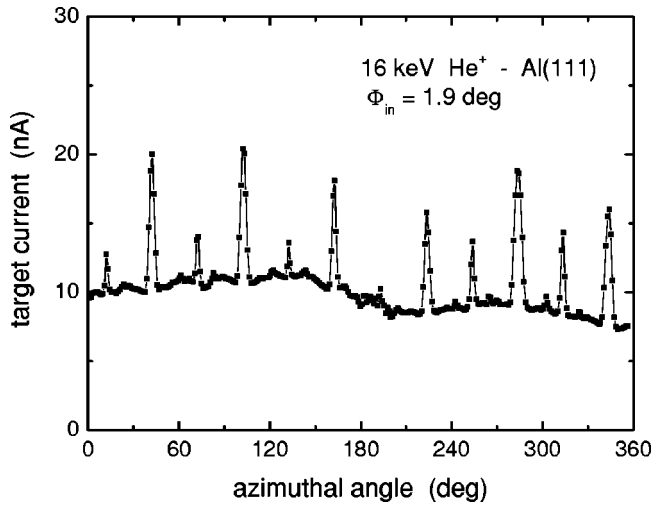


FIG. 1. Target current as function of azimuthal angle for scattering of 16 keV He⁺ ions from Al(111) under $\Phi_{in} = 1.9^\circ$.

beams of fast He^o atoms (He⁺ beam chopped by electric-field plates and neutralized in gas target) hit the sample under an azimuthal angle Θ_{in} , and specularly reflected projectiles are recorded by means of a channelplate electron multiplier. Electrons emitted from the Al surface are collected by a weak electric field owing to a bias of some 10 V applied to a highly transparent grid about 1 cm in front of the target and accelerated onto the SBD. Because the efficiency of the electron detector is close to 100%,¹⁶ corrections of measured SBD pulse heights with respect to electron detection loss can be neglected here. Details on our experimental setup can be found elsewhere.¹⁷

In Fig. 1 we show the (uncompensated) target current for scattering of 16 keV He⁺ ions from Al(111) under $\Phi_{in} = 1.9^\circ$ as function of the azimuthal angle Θ . This current shows peaks for scattering along low index crystallographic directions. The prominent peaks are assigned to $\langle 110 \rangle$ directions showing the sixfold symmetry of the (111) surface. In intervals of 30° between these peaks we find less pronounced peaks for scattering along $\langle 211 \rangle$ strings. The widths of the peaks are determined by the critical angles for axial channeling which scale with d^{-1} , d being the spacing between adjacent atoms of strings.^{3,5,10} This spacing grows with increasing crystallographic index and explains the decrease of the experimental widths with increasing index. Curves as displayed in Fig. 1 are well established and were interpreted in former work by enhanced electron densities probed by projectiles and/or longer trajectories.^{6-8,10,15}

For a more detailed investigation on this problem, we have recorded electron number distributions for 16 keV He^o impact at different azimuthal angles Θ . These spectra are taken (1) coincident and (2) noncoincident with projectiles reflected specularly within the acceptance angle of the multichannelplate detector; i.e., for (1) we detect only those events related to near-perfect scattering from primarily the topmost surface, whereas for (2) emission events for all projectiles are recorded.

In the first part of our experiments, we performed studies for scattering under planar surface channeling, i.e., “ran-

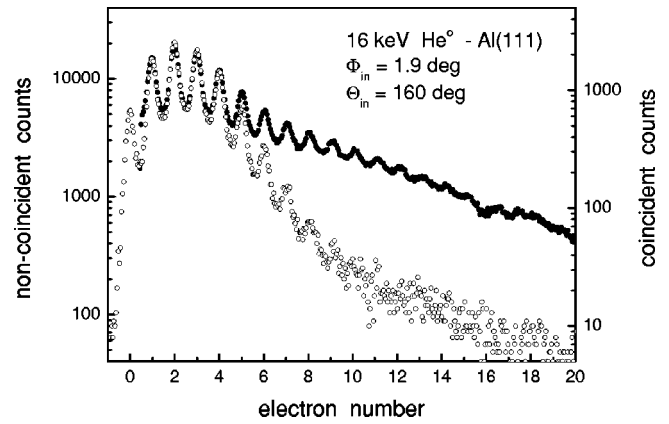


FIG. 2. Coincident (open circles) and noncoincident (full circles) electron number spectra for scattering of 16 keV He^o atoms from Al(111) under $\Phi_{in} = 1.9^\circ$ and $\Theta_{in} = 160^\circ$.

dom” azimuthal alignment of the target surface. In Fig. 2 we show in a semilogarithmic plot coincident (open circles) and noncoincident (full circles) SBD spectra for 16 keV He^o projectiles. For comparison, the substantial noise of the SBD (cf. Fig. 3) is subtracted in the noncoincident spectra, whereas in the coincident data peak heights within the noise level represent events related to the emission of no electron.¹⁷ Normalization of spectra to same peak heights at low electron number reveals a pronounced tail for noncoincident detection. We attribute this tail to a fraction of projectiles which have penetrated into the near surface region of the bulk of the Al target and excite a fair number of electrons including cascades of electrons. Penetration into the bulk will be mediated by surface imperfections and thermal vibrations of target atoms. Electron emission in this regime is clearly more efficient than emission induced by specularly reflected projectiles as monitored in coincident detection. By translation of the target into the incident beam we checked that the tail in the noncoincident spectra is not related to projectiles which hit the front side of the target as observed at high projectile energies for an insulator surface by Andou *et al.*¹⁵

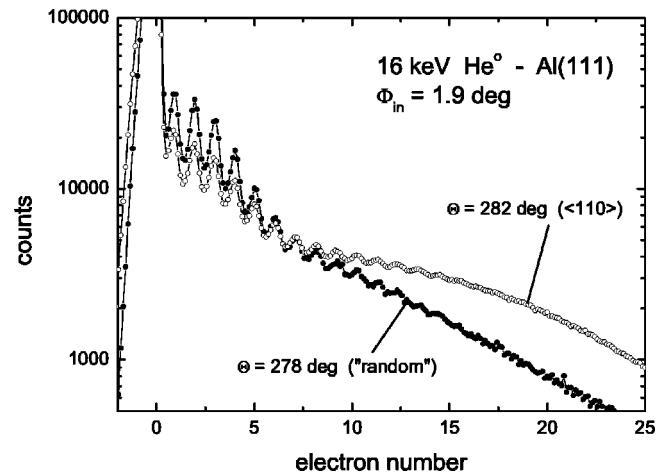


FIG. 3. Noncoincident electron number spectra for scattering of 16 keV He^o atoms from Al(111) under $\Phi_{in} = 1.9^\circ$ and $\Theta_{in} = 282^\circ$ (open circles), and 278° (full circles).

In the second part of our work we recorded electron number spectra for axial surface channeling conditions. It turns out that noncoincident spectra are of special interest here, since these spectra stem from impact of all projectiles and can be directly related to measurements of the target current. In Fig. 3 we compare electron number spectra where scattering proceeds under random and under axial surface channeling. Note the spectra are not corrected for SBD noise, giving rise to the pronounced peak at zero electron number.

The noncoincident spectra (normalized to same number of events for $n > 1$) in Fig. 3 reveal a different behavior of the count rates for low (about $n \leq 4$) and higher electron number n . Whereas for low n the influence of a transition from planar to axial channeling is an overall reduction of intensities by about 20%, we observe a pronounced difference of intensity at higher n . Although integral intensities of the spectra are dominated by events resulting in emission of only a few electrons, i.e., induced by the majority of projectiles scattered from the surface plane, projectiles penetrating into the subsurface region provide substantial contributions to the overall electron emission yields owing to a much larger number of electrons emitted per projectile impact.

This interpretation is consistent with coincident time-of-flight spectra. For axial channeling small contributions with clearly higher projectile energy loss appear which are related to a larger number of emitted electrons. These events stem from projectiles which emerge from subsurface scattering to vacuum and reach the detector. The enhanced penetration of projectiles under axial surface channeling conditions can be understood in terms of a steering effect by strings of atoms so that projectiles reach adjacent strings in subsurface layers. Those trajectories are suppressed under planar channeling for random orientation.

This interaction scenario clearly differs from the former understanding of this effect where the majority of projectiles contributes to the enhancement of electron yields. Then a shift of the prominent peaks at low electron numbers to higher values is expected. However, this feature is not observed in the spectra.

For a direct comparison of electron number spectra and target current we derive from the number spectra electron emission yields γ for coincident as well as noncoincident detection from measured probabilities W_n for the emission of n electrons.^{16,17} In Fig. 4 we show a bar graph of total electron yields for selected azimuthal angles Θ . The hatched and open parts of the bars represent coincident and noncoincident contributions of the total yields, respectively. Note that only the noncoincident fractions show an increase for axial channeling, whereas the coincident yields are hardly affected. The dots connected by a solid curve represent the target current for 16 keV He⁺ ions scattered under $\Phi_{in} = 1.9^\circ$ which is basically the sum of the current from incoming ions and emitted electrons. Thus, aside from a constant pedestal, the target current is proportional to the electron yields so that the scales for target current and total electron yields can be matched. Although much higher fluxes for He ions than for atoms were necessary and a slight overall increase of total

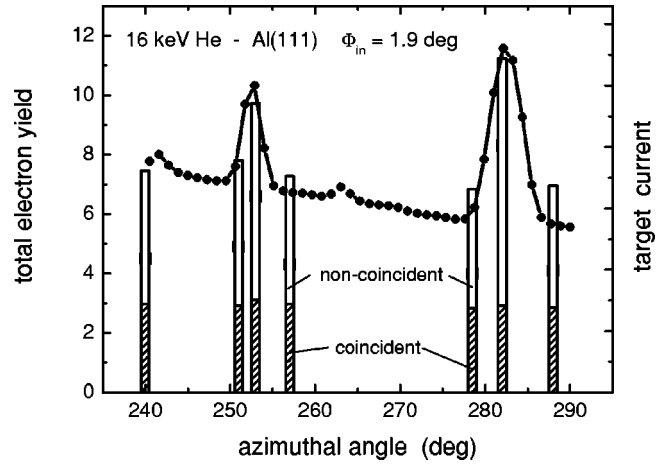


FIG. 4. Target current (He⁺ impact, full circles) and total electron yields (He atoms, hatched bars = coincident detection, open bars = noncoincident detection) for scattering of 16 keV He⁺/He⁰ from Al(111) under $\Phi_{in} = 1.9^\circ$.

yields due to potential emission for ions is present, the agreement between both measurements is fairly good and supports our interpretation of data.

Our experimental technique and the new understanding of the interaction mechanisms bear the potential of an application for “ion beam triangulation.”¹⁴ Since the peaks observed for scattering along low-index strings of atoms are attributed to a small portion of projectiles producing a comparably much larger number of electrons during their stopping in the subsurface layer, one can enhance the effect by a selection of events for the emission of a higher number of electrons. In Fig. 5 we show count rates from the SBD as function of the azimuthal angle Θ for two different discriminator pulse height levels.

For a discriminator level of $U_{disc} = 0.15$ V we only suppress the noise of the SBD pulses for noncoincident detection. Since, irrespective of projectile trajectories, most projectiles produce at least one electron, the count rates of the

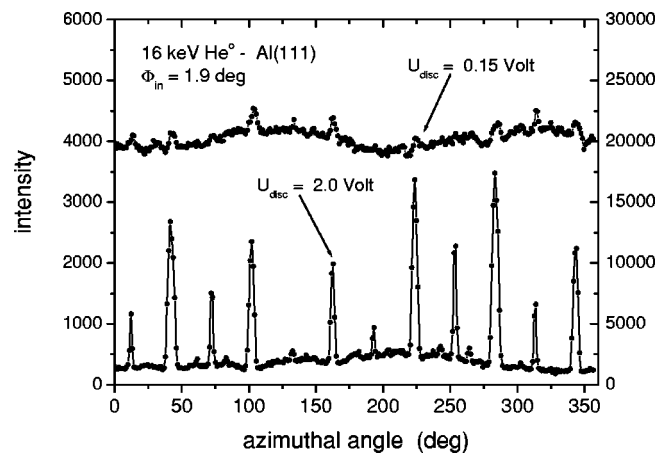


FIG. 5. SBD count rate as function of azimuthal angle for scattering of 16 keV He⁰ atoms from Al(111) under $\Phi_{in} = 1.9^\circ$. Upper curve: discriminator level $U_{disc} = 0.15$ V, lower curve $U_{disc} = 2.0$ V.

SBD show only a small effect on a variation of Θ (upper curve). For $U_{disc}=2.0$ V, events related to the emission of more than about nine electrons are selected (lower curve). The relative peak height for a transition from planar to axial surface channeling is increased here by a factor of up to about 10, whereas the target current is enhanced by a factor of about 2 only (cf. Fig. 1). We propose to make use of electron number spectra for studies on the structure of surfaces and thin films with a high signal to background ratio. Since the overall detection efficiency for counting electrons with our setup is close to one, only about 1000 projectiles per second have to be directed onto the target surface (compared to some tens of nanoampere in order to produce data as displayed in Fig. 1). Then effects of radiation damage induced by scattered projectiles at the target are on a negligible level which is relevant for studies on the structure of ultrathin films and species weakly bound to the surface.

In conclusion, we have clarified important features for kinetic electron emission under axial surface channeling. Electron number spectra reveal that the observed enhancement of total electron yield stems from a fraction of projectiles which have penetrated into the subsurface region. This knowledge can be used to improve the signal-to-background ratio in ion beam triangulation studies as a tool for structural studies of ultrathin films. We hope that our work stimulates theoretical treatments on the detailed emission processes which comprise the description of projectile trajectories, electron excitation processes, and electron transport phenomena.

We thank D. Blauth for his assistance in the experiments and the DFG (Project No. Wi 1336 and Sonderforschungsbereich 290, Teilprojekt A7) and Austrian FWF (Project No. 14337) for support.

*Corresponding author; Electronic address: winter@physik.huberlin.de

¹M.T. Robinson and O.S. Oen, Phys. Rev. **132**, 2385 (1963).

²J.A. Davies, Phys. Scr. **28**, 294 (1983).

³D. Gemell, Rev. Mod. Phys. **46**, 129 (1974).

⁴M. W. Thompson, in *Channeling*, edited by D. V. Morgan (Wiley, London, 1973), p. 1.

⁵R. Sizmann and C. Varelas, Nucl. Instrum. Methods **132**, 633 (1976).

⁶H. Winter, Phys. Rep. **367**, 387 (2002).

⁷M. Hasegawa, K. Kimura, Y. Fujii, M. Suzuki, Y. Susuki, and M. Mannami, Nucl. Instrum. Methods Phys. Res. B **33**, 334 (1988).

⁸H. Winter, G. Dierkes, A. Hegmann, J. Leuker, H.W. Ortjohann, and R. Zimmy, in *Ionization of Solids by Heavy Particles*, Vol. 306 of *NATO ASI Series B: Physics*, edited by R. A. Baragiola (Plenum Press, New York, 1993), p. 253.

⁹G. Spierings, I. Urazgildin, P.A. Zeijlmans van Emmichoven, and

A. Niehaus, Phys. Rev. Lett. **74**, 4543 (1995).

¹⁰H. Winter, Ph.D. thesis, Munich, 1986 (author not identical with two authors of this paper).

¹¹C. Lemell, J. Stöckl, HP. Winter, and F. Aumayr, Rev. Sci. Instrum. **70**, 1653 (1999).

¹²N. Benazeth, Nucl. Instrum. Methods Phys. Res. **194**, 405 (1982).

¹³J. Schou, Scan Electron Microsc. **2**, 44 (1988).

¹⁴R. Pfandzelter, T. Bernhard, and H. Winter, Phys. Rev. Lett. **90**, 036102 (2003).

¹⁵G. Andou, K. Nakajima, and K. Kimura, Nucl. Instrum. Methods Phys. Res. B **160**, 16 (2000).

¹⁶G. Lakits, F. Aumayr, and HP. Winter, Rev. Sci. Instrum. **60**, 3151 (1989).

¹⁷A. Mertens, K. Maass, S. Lederer, H. Winter, J. Eder, J. Stöckl, HP. Winter, F. Aumayr, J. Vieffhaus, and U. Becker, Nucl. Instrum. Methods Phys. Res. B **182**, 23 (2001).